

See discussions, stats, and author profiles for this publication at: <https://www.researchgate.net/publication/228498348>

Investigation of the Surface Morphology and Photoisomerization of an Azobenzene-Containing Ultrathin Film

ARTICLE *in* LANGMUIR · APRIL 1996

Impact Factor: 4.46 · DOI: 10.1021/la950943n

CITATIONS

54

READS

9

6 AUTHORS, INCLUDING:



Rong Wang

Illinois Institute of Technology

55 PUBLICATIONS 4,469 CITATIONS

SEE PROFILE



Leiwen Jiang

National Research Center (CO, USA)

72 PUBLICATIONS 1,394 CITATIONS

SEE PROFILE



Donald A. Tryk

University of Yamanashi

250 PUBLICATIONS 15,559 CITATIONS

SEE PROFILE



Kenkichi Hashimoto

Kyushu Medical Center

499 PUBLICATIONS 14,566 CITATIONS

SEE PROFILE

Investigation of the Surface Morphology and Photoisomerization of an Azobenzene-Containing Ultrathin Film

R. Wang,^{†,‡} L. Jiang,^{†,‡} T. Iyoda,[‡] D. A. Tryk,[†] K. Hashimoto,^{†,‡} and A. Fujishima^{*,†,‡}

Department of Applied Chemistry, Faculty of Engineering, The University of Tokyo, Hongo, Bunkyo-ku, Tokyo 113, Japan, and the Photochemical Conversion Materials Project, Kanagawa Academy of Science and Technology, 1583 Iiyama, Atsugi, Kanagawa 243-02, Japan

Received October 27, 1995[®]

Atomic force microscopy (AFM) and Fourier transform infrared (FTIR) spectroscopy were used to investigate the structure and surface morphology of an azobenzene-containing Langmuir–Blodgett (LB) film. Molecularly-resolved AFM images revealed a slightly distorted monoclinic crystal structure with a unit cell of $a = 6.08 \pm 0.03$ Å, $b = 5.67 \pm 0.03$ Å, and an angle of $55^\circ \pm 1^\circ$ between these two in-plane axes. An average molecular orientation of $39^\circ \pm 2^\circ$ with respect to the film surface normal was determined using FTIR spectra. Using polarized UV excitation of the azobenzene-containing LB film, selective trans-to-cis photoisomerization was obtained and was characterized by the polarized UV–visible spectra. Clear morphological differences between films subjected to unpolarized vs polarized UV illumination were observed with in situ AFM. Domains on the order of 10 nm in diameter or less are thought to be associated with the photoisomerization process.

Introduction

Organic materials whose optical properties can be varied locally and in a reversible way by light have enormous potential for use in electro-optic and opto-optic devices.^{1–5} Azobenzene derivatives are particularly promising candidates and have been widely investigated for the past few decades because of their reversible trans–cis photoisomerization and electrochemical activity.^{6–10} The Langmuir–Blodgett (LB) technique has been shown to be a powerful, convenient method for the preparation of ultrathin, uniform, and controllable films. Such films offer an interesting opportunity for the study of the physical and chemical properties, such as pyroelectricity,¹¹ phase transitions,¹² aggregation effects,¹³ and so on, at a molecular level.

The use of linearly polarized light offers a fundamentally new approach to induce in-plane anisotropy in assembled

photochromic films. Surface photoregulation of liquid crystal alignment,^{14–16} photoinduced reorientation,^{17–20} linear photopolymerization,²¹ birefringence,^{22,23} and in-plane anisotropic photobleaching^{17,24} has been reported to be effectively controllable using polarized irradiation. In addition to spectroscopy, the investigation of real-space structural variations is becoming a major concern for these processes. Atomic force microscopy (AFM) provides a nondestructive means for imaging the surfaces of ultrathin films at molecular resolution^{25–27} and monitoring structural conversions due to UV excitation.^{28,29}

Recently, we have developed a new type of in-plane (film surface plane) selective interconversion process utilizing successive polarized UV irradiation steps incorporating a photochemical/electrochemical hybrid technique.^{30,31} Azobenzene-containing amphiphilic molecules, which

* To whom correspondence should be addressed. Telephone: +81-3-3812-9276. Fax: +81-3-3812-6227. E-mail: fujishima@tansei.cc.u-tokyo.ac.jp.

[†] The University of Tokyo.

[‡] Photochemical Conversion Materials Project, KAST Lab.

[®] Abstract published in *Advance ACS Abstracts*, April 1, 1996.

(1) Willner, I.; Blonder, R.; Dagan, A. *J. Am. Chem. Soc.* **1994**, *116*, 9365.
(2) Gibbons, W. M.; Shannon, P. J.; Sun, S. T.; Swetlin, B. J. *Nature* **1991**, *351*, 49.

(3) Saika, T.; Iyoda, T.; Honda, K.; Shimidzu, T. *J. Chem. Soc., Chem. Commun.* **1992**, 591.

(4) Karatsu, T.; Shiga, T.; Kitamura, A.; Arai, T.; Sakuragi, H.; Tokumaru, K. *Chem. Lett.* **1994**, 825.

(5) Kajikawa, K.; Anzai, T.; Takezoe, H.; Fukuda, A. *Thin Solid Films* **1994**, *243*, 587.

(6) Sekkat, Z.; Büchel, M.; Orendi, H.; Menzel, H.; Knoll, W. *Chem. Phys. Lett.* **1994**, *220*, 497.

(7) Maack, J.; Ahuja, R. C.; Möbius, D.; Tachibana, H.; Matsumoto, M. *Thin Solid Films* **1994**, *242*, 122.

(8) Knobloch, H.; Orendi, H.; Büchel, M.; Sawodny, M.; Schmidt, A.; Knoll, W. *Fresenius' J. Anal. Chem.* **1994**, *349*, 107.

(9) Herr, B. R.; Mirkin, C. A. *J. Am. Chem. Soc.* **1994**, *116*, 1157.

(10) Liu, Z. F.; Hashimoto, K.; Fujishima, A. *Nature* **1990**, *347*, 658.

(11) Wang, R.; Yang, J.; Wang, H.; Tang, D. X.; Jiang, L.; Li, T. *J. Thin Solid Films* **1995**, *256*, 205.

(12) Kawai, T.; Umemura, J.; Takenaka, T. *Langmuir* **1989**, *5*, 1378.

(13) Xu, X. F.; Era, M.; Tsutsui, T.; Saito, S. *Thin Solid Films* **1989**, *178*, 541.

(14) Akiyama, H.; Momose, M.; Ichimura, K.; Yamamura, S. *Macromolecules* **1995**, *28*, 288.

(15) Ikeda, T.; Tsutsumi, O. *Science* **1995**, *268*, 1873.

(16) Seki, T.; Sakuraki, M.; Suzuki, Y.; Tamaki, T.; Fukuda, R.; Ichimura, K. *Langmuir* **1993**, *9*, 211.

(17) Yokoyama, S.; Kakimoto, M.; Imai, Y. *Langmuir* **1994**, *10*, 4594.

(18) Menzel, H.; Weichert, B.; Schmidt, A.; Paul, S.; Knoll, W.; Stumpe, J.; Fischer, T. *Langmuir* **1994**, *10*, 1926.

(19) Möbius, G.; Pietsch, U.; Geue, Th.; Stumpe, J.; Schuster, A.; Ringsdorf, H. *Thin Solid Films* **1994**, *247*, 235.

(20) Anderle, K.; Birenheide, R.; Eich, M.; Wendorff, J. H. *Makromol. Chem., Rapid Commun.* **1989**, *10*, 477.

(21) Schadt, M.; Schmitt, K.; Kozinkov, V.; Chigrinov, V. *Jpn. J. Appl. Phys.* **1992**, *31*, 2155.

(22) Ramanujam, P. S.; Hvilsted, S.; Andruzzi, F. *Appl. Phys. Lett.* **1993**, *62* (10), 1041.

(23) Shi, Y.; Steier, W. H.; Yu, L.; Chen, M.; Dalton, L. R. *Appl. Phys. Lett.* **1991**, *59*, 2935.

(24) Yokoyama, S.; Kakimoto, M.; Imai, Y. *Langmuir* **1993**, *9*, 1086.

(25) Meyer, E.; Howald, L.; Overney, R. M.; Heinzelmann, H.; Frommer, J.; Güntherodt, H. J.; Wagner, T.; Scher, H.; Roth, S. *Nature* **1991**, *349*, 398.

(26) Caldwell, W. B.; Campbell, D. J.; Chen, K.; Herr, B. R.; Mirkin, C. A.; Malik, A.; Durbin, M. K.; Dutta, P.; Huang, K. G. *J. Am. Chem. Soc.* **1995**, *117*, 6071.

(27) Wolf, H.; Ringsdorf, H.; Delamarche, E.; Takami, T.; Kang, H.; Michel, B.; Gerber, Ch.; Jaschke, M.; Butt, H.-J.; Bamberg, E. *J. Phys. Chem.* **1995**, *99*, 7102.

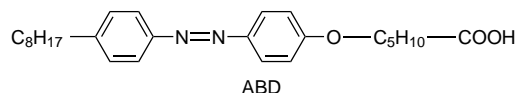
(28) Schönhoff, M.; Chi, L. F.; Fuchs, H.; Lösche, M. *Langmuir* **1995**, *11*, 163.

(29) Umemoto, T.; Ishikawa, K.; Takezoe, H.; Fukuda, A.; Sasaki, T.; Ikeda, T. *Jpn. J. Appl. Phys.* **1993**, *32*, L936.

undergo the $\text{trans} \rightarrow \text{cis} \rightarrow \text{hydrazobenzene}$ photoelectrochemical conversion reaction, have transition moments for the azobenzene $\pi-\pi^*$ transition whose projections in the LB film surface are parallel to the polarization plane of the UV illumination beam. The interconversion has been induced successively and selectively along different polarization directions in the same microscopic area. Interestingly, spectroscopic study reveals that the orientations of the trans -isomers in different directions remain unchanged for short exposure to polarized UV irradiation.³⁰ On prolonged UV irradiation with polarized light, selective $\text{trans} \rightarrow \text{cis}$ photoisomerization is also found in the film although it is accompanied by a reorientation process for the isomerized molecules.³¹ Such a phenomenon allows the assumption that the unreacted molecules may be to some extent independent of the reacted molecules. In order to better understand this interconversion process, in the present work, we have focused on the studies of the structure and the structural variations in anisotropically photoisomerizable LB films containing the azobenzene moiety. It is proposed that the in-plane selectivity of the photoisomerization process is associated with the domains in the film.

Experimental Section

Sample Preparation. The amphiphilic azobenzene derivative (ABD) 4-octyl-4'-(5-carboxypentamethyleneoxy)azobenzene, whose molecular structure is



was purchased from Dojindo Laboratory (Kumamoto, Japan). The ABD was dissolved in chloroform to obtain a spreading solution of concentration 1.8×10^{-3} M.

The films were assembled on the air–water interface of a thermostated LB trough (USI). Deionized, Millipore-purified water containing 2×10^{-4} M CdCl_2 was used as the subphase. At a subphase temperature of 20°C , the ABD chloroform solution was spread dropwise at the air–water interface. After 20 min to allow the chloroform to evaporate, the film was slowly compressed at a constant barrier speed of $0.15 \text{ cm}^2/\text{s}$. The monolayer film was transferred onto CaF_2 plates using a conventional vertical dipping LB technique at a surface pressure of 25 mN/m , corresponding to a molecular area of 29.8 \AA^2 . Multilayer films were fabricated in a head-to-tail (Y-type) manner. Prior to deposition, the CaF_2 plates were cleaned by alternative ultrasonication in ethanol and chloroform for 10 min each. The procedures for the LB film preparation were carried out under dim red light conditions in order to ensure that all of the azobenzene moieties were in the trans form. In order to facilitate the comparison of results obtained using different methods, all of the studies in the present work were carried out with nine-layer films.

Apparatus. AFM investigations were conducted using a commercial system (Seiko Instruments Inc., SPA300) with a $20 \text{ }\mu\text{m}$ scanner. All images were recorded under ambient conditions ($22\text{--}23^\circ\text{C}$, 60% relative humidity). A triangular-shaped Si_3N_4 cantilever with a spring constant of 0.02 N/m was used to acquire images in the contact mode. The force between the tip and the sample was typically 1 nN . Noncontact mode measurements were performed using a rectangular-shaped Si_3N_4 cantilever with a spring constant of 0.09 N/m . The molecularly resolved images were acquired in contact mode with “constant height” measurement, at a scan rate of 16.27 Hz . Besides the raw image, a Fourier-filtered image was obtained to emphasize the periodic feature of the raw image. The program used to calculate the fast Fourier transform (FFT) itself was supplied by Seiko Instrument

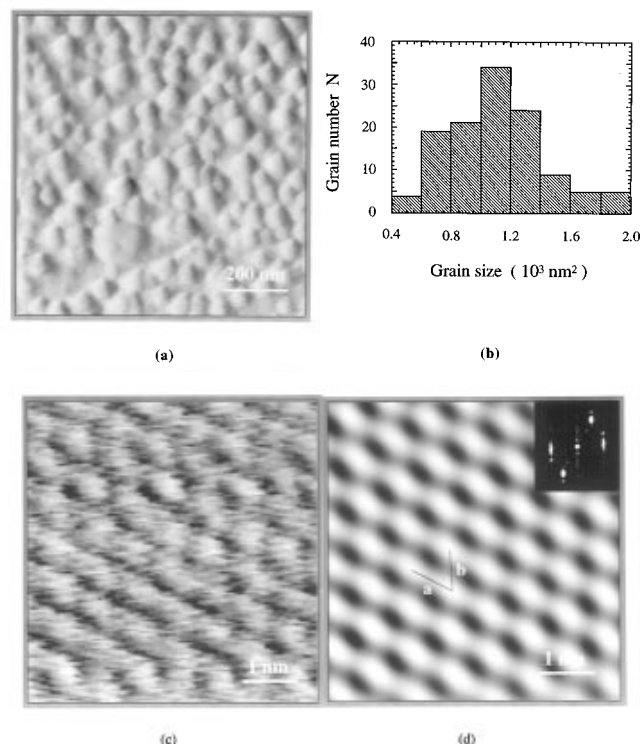


Figure 1. AFM images of a freshly prepared nine-layer ABD LB film on a CaF_2 substrate: (a) large-scale image of grain structure in the film ($800 \text{ nm} \times 800 \text{ nm}$, “constant height” in contact mode); (b) distribution of the grain sizes of 120 grains. The areas were determined from AFM images in (a) and other typical AFM images; (c) raw molecular scale image ($5 \text{ nm} \times 5 \text{ nm}$, “constant height” in contact mode) obtained on top of a large grain in (a); (d) enhanced image (Fourier-filtered) and Fourier transform (inset) of (c) (see text for details). The nearest-neighbor spacings estimated from the FFT data are $a = 6.08 \pm 0.03 \text{ \AA}$ and $b = 5.67 \pm 0.03 \text{ \AA}$, respectively.

Co. The pronounced frequency pattern in the FFT spectrum was reversely transformed to the filtered image. Large-scale images were acquired in either contact mode or noncontact mode with both “constant height” and “constant force” measurements. The scan speed was $2.03\text{--}4.07 \text{ Hz}$. After polarized and unpolarized UV irradiation, AFM images were recorded for comparison with the surface morphology of the freshly prepared film.

Linear dichroic FTIR transmission spectra were recorded on a JASCO FT/IR-8900 spectrophotometer equipped with a wire-grid polarizer. Spectra were taken at 4 cm^{-1} resolution with 500-scan accumulation for an acceptable signal/noise ratio.

Polarized UV–visible spectra of the ABD film before and after polarized UV irradiation were recorded on a Shimadzu UV-3101PC UV–visible spectrophotometer with dichroic sheet polarizers. Unpolarized UV irradiation was carried out using a xenon lamp with an optical fiber coupler, employing two band-pass filters to obtain light with a wavelength of 365 nm for the $\text{trans} \rightarrow \text{cis}$ photoisomerization at a photointensity of 18.5 mW/cm^2 on the sample. The dichroic sheet polarizer was set between the lamp and the sample to obtain the desired polarized UV irradiation with a photointensity of 4.5 mW/cm^2 on the sample.

Results and Discussion

Film Structure. Typical AFM images of a freshly prepared nine-layer film on a CaF_2 substrate are shown in Figure 1. Randomly distributed grains are clearly visible in the low-resolution image (Figure 1a). The grains are not uniform in size on the surface. The areas of 120 grains in this and other AFM images were measured. The size distribution (Figure 1b) shows that the grains have an average area of $1100 \pm 25 \text{ nm}^2$. The average thickness of the grains is $27 \pm 1 \text{ \AA}$, corresponding to approximately one ABD monolayer.

(30) Wang, R.; Iyoda, T.; Hashimoto, K.; Fujishima, A. *J. Phys. Chem.* **1995**, *99*, 3352.

(31) Wang, R.; Iyoda, T.; Hashimoto, K.; Fujishima, A. *J. Photochem. Photobiol., A: Chem.* **1995**, *92*, 111.

The flat facets on top of the relatively large grains are adequate for observation of the ordered packing of the LB film. Figure 1c shows a raw high-resolution AFM image obtained on top of a large grain, illustrating the characteristics of the ABD LB film surface. The enhanced image (FFT spectrum filtered) of Figure 1c is shown in Figure 1d. The ABD molecules are arranged regularly with intermolecular distances of 6.08 ± 0.03 and 5.67 ± 0.03 Å along the *a* and *b* axes, respectively, as indicated in Figure 1d, and the angle between the two axes is $55^\circ \pm 1^\circ$. These values were measured from the two-dimensional FFT of the image (see inset). The FFT pattern was calculated from the raw ABD image. It shows different spacings along the two in-plane axes, indicating a slightly distorted monoclinic crystal structure.^{25,32,33} The packing density (area per molecule) of 30.4 ± 0.5 Å², calculated from the Fourier pattern in Figure 1d, is in reasonable agreement with the value obtained from the π -A curve (29.8 Å²). The film thickness of 233 ± 5 Å was measured at the film boundary, indicating an average thickness of 25.9 ± 0.5 Å for each monolayer.

AFM images allow only the study of the two-dimensional molecular arrangement on the film surface. FTIR spectroscopy has been widely accepted as an effective tool to determine the orientations of the long axes and the functional groups of molecules with respect to the surface normal of LB films.^{34,35} By combining the data from AFM with the results of FTIR spectra, three-dimensional molecular arrangements can be deduced.

Figure 2 gives the linearly polarized FTIR transmission spectra (a) of a nine-layer ABD film on a CaF₂ plate as well as a diagrammatic sketch depicting the orientation of the transition dipole moment (b). When the polarized IR beam is introduced along the film surface normal, with the polarization direction either parallel ($A_{||}(i=0^\circ)$) or perpendicular ($A_{\perp}(i=0^\circ)$) to the film-dipping direction, the spectra show different absorption intensities at frequencies associated with specific vibrational modes. The dichroic feature indicates that the molecular projections on the film surface are anisotropically oriented. The anisotropy is evaluated by an angle ω relative to the film-dipping direction, which is defined by³⁴

$$\langle \cos 2\omega \rangle = |A_{||}(i=0^\circ) - A_{\perp}(i=0^\circ)| / [A_{||}(i=0^\circ) + A_{\perp}(i=0^\circ)] \quad (1)$$

where $A_{||}(i=0^\circ)$ and $A_{\perp}(i=0^\circ)$ are the transmission absorbances in the two orthogonal directions. The Φ parameter (see Figure 2b) is also determined to give important information on molecular orientation. Linearly polarized light, with the electric field parallel to the plane of incidence, is applied to the film surface with incident angles of 0° and 30° , respectively. The corresponding absorbances ($A_{\perp}(i=0^\circ)$ and $A_{\perp}(i=30^\circ)$) are different due to the uniaxial orientation of the transition moment for each vibration mode at an angle Φ from the film surface normal. The angle Φ is predominantly determined by $A_{\perp}(i=0^\circ)$, $A_{\perp}(i=30^\circ)$, and $A_{||}(i=0^\circ)$, as shown by Vandevyver et al.³⁴ The FTIR spectra in Figure 3 allow us to estimate the average orientations ω and Φ of the typical transition dipole moments, as shown in Table 1. It should be noted that the angle Φ represents the average orientation of the relevant transition moment, whereas the angle ω is just

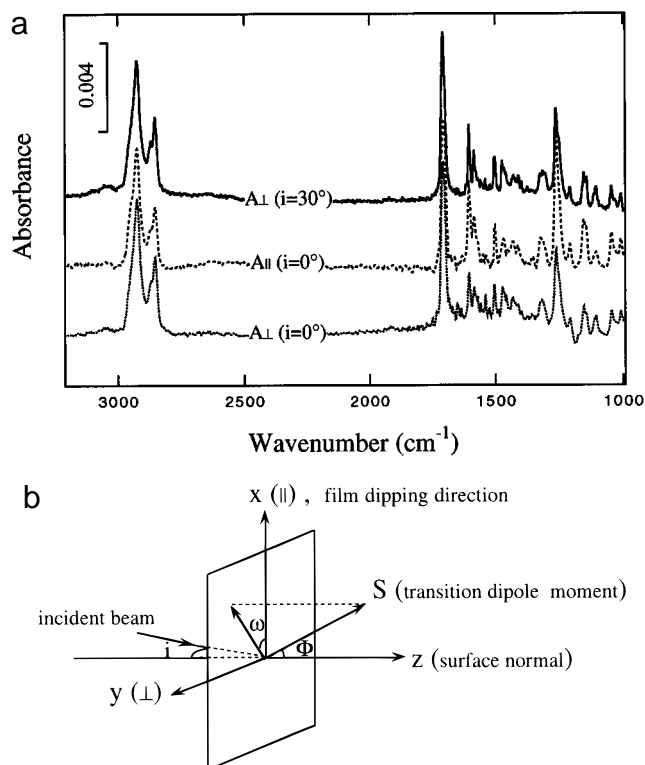


Figure 2. Linear dichroic FTIR spectra of a freshly prepared nine-layer ABD film on a CaF₂ substrate (a) and diagrammatic sketch showing the transition dipole moment related to i , ω , and Φ (b). In (a), spectra are shown with the electric field parallel to the plane of incidence, the linearly polarized light arriving onto the film at normal incidence ($A_{\perp}(i=0^\circ)$) and at an angle of 30° ($A_{\perp}(i=30^\circ)$) relative to the film surface normal, as well as with the electric field perpendicular to the plane of incidence, the linearly polarized light arriving onto the film at normal incidence ($A_{||}(i=0^\circ)$).

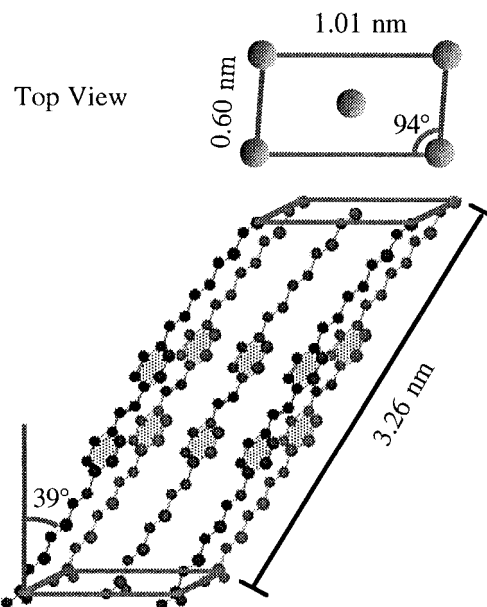


Figure 3. Slightly distorted monoclinic unit cell in the ABD film.

used to estimate the in-plane anisotropy as defined in eq 1. The tilt angle of the aliphatic chain is determined by examining the asymmetric CH₂ stretching band at 2925 cm⁻¹ and the symmetric CH₂ stretching band at 2854 cm⁻¹.³⁵ The tilt angle of the long axis of the *trans*-azobenzene moiety is calculated from the average orientation of the transition dipole moments of the 1604 cm⁻¹

(32) Snyder, R. G. *J. Chem. Phys.* **1979**, *71*, 3229.

(33) Koyama, Y.; Yanagishita, M.; Toda, S.; Matsuo, T. *J. Colloid Interface Sci.* **1977**, *61*, 438.

(34) Vandevyver, M.; Barraud, A.; Teixier, R.; Maillard, P.; Gianotti, C. *J. Colloid Interface Sci.* **1982**, *85*, 571.

(35) Umemura, J.; Kamata, T.; Kawai, T.; Takenaka, T. *J. Phys. Chem.* **1990**, *94*, 62.

Table 1. Orientation of the Chain Axis and Various Transition Moments of ABD in a Nine-Layer LB Film

vibration mode	peak position (cm ⁻¹)	orientation		tilt angle of the aliphatic chain (deg)
		ω (deg)	Φ (deg)	
$\nu_s(\text{CH}_2)$	2923	44	68	} 39
$\nu_{as}(\text{CH}_2)$	2854	43	59	
$\nu(\text{benzene})$ (longest benzene axis)	1604	38	35	
$\nu(\text{benzene}-\text{O})$	1262	37	39	}
$\nu(\text{N}-\text{benzene})$	1153, 1143	38	39	

band (in-plane vibration of the benzene ring along the long axis of the azobenzene moiety), the 1262 cm⁻¹ band (benzene-O stretching), as well as the 1153 and 1143 cm⁻¹ bands (benzene-N stretching).^{36,37} As indicated by the values for ω listed in Table 1, the projections of the aliphatic chains in the film surface plane exhibit an isotropic distribution. In contrast, the projections of the azobenzene moieties are distributed anisotropically, with an average angle of $38^\circ \pm 2^\circ$, indicating a projection of the azobenzene moieties on the film surface with a preferential orientation along the film-dipping direction. Considering the values of Φ in Table 1, the aliphatic chains exhibit a tilt angle of $39^\circ \pm 2^\circ$ with respect to the film surface normal, and the azobenzene functional groups also exhibit a similar angle, $38^\circ \pm 2^\circ$. The inclination of the molecules results in a considerable projection of the transition moment of the azobenzene moiety in the film surface plane, which provides the opportunity for the polarized photoisomerization.¹⁷

Incorporating the surface morphology from the AFM image and the orientation from the FTIR spectra, a three-dimensional monoclinic unit cell for the ABD LB film is proposed (Figure 3). The intermolecular distances and angles were estimated from the FFT data in Figure 1d. The tilt angles of the aliphatic chains and the azobenzene functional groups relative to the film surface normal were obtained from the FTIR spectra. The individual length of an ABD molecule is 32.6 Å.³⁹ As mentioned previously, a thickness of 233 ± 5 Å was measured at the edge of a nine-layer LB film. This allows us to estimate the average tilt angle of the molecules in the film at about $37^\circ \pm 2^\circ$, which is consistent with the value derived from the FTIR spectra. From the above results, it is inferred that the ABD molecules in the LB film are highly tilted, with a slightly distorted monoclinic crystal structure. The projections of the ABD molecules in the film surface plane are distributed along the different in-plane directions, with a preferential orientation in the film-dipping direction. Taking advantage of the inclined molecular axis, in-plane observation of the trans \rightarrow cis photoisomerization is possible due to the large projection of the transition moment of the azobenzene moiety on the film surface.

In-Plane Selective Photoisomerization. Excitation by linearly polarized UV light causes the ABD LB film to undergo an anisotropic photoisomerization.³⁰ Polarized UV-visible spectroscopy provides a powerful means to monitor the selective conversion process. Figure 4 shows the in-plane polarized UV-visible spectra of a nine-layer film of ABD on a CaF₂ substrate before and after linearly polarized UV irradiation. Regarding the coordinate system in Figure 2b, the film surface is in the *xy* plane, and the probe light beam was polarized either in the *xy* plane (||) or in the *yz* plane (⊥). The in-plane anisotropic

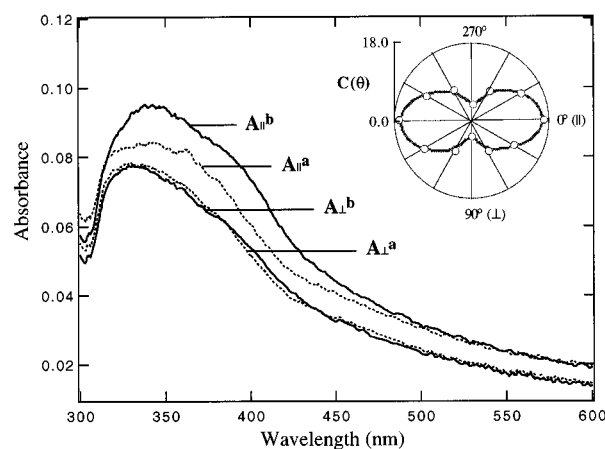


Figure 4. Polarized UV-visible spectra of a nine-layer ABD film after a 2.5 min polarized UV irradiation, with the polarization plane parallel to the film-dipping direction. $A_{||}^b$ (or $A_{||}^a$) and A_{\perp}^b (or A_{\perp}^a) correspond to the absorbances of the film with polarizers aligned parallel and perpendicular to the film-dipping direction before (or after) the irradiation, respectively. The inset is the polar plot for the polarized photoreaction parameter $C(\theta)$ depicted as the vector length vs the angle between the plane of polarization of the incident probe beam and the film-dipping direction. $\theta = 0^\circ$ was defined when the polarizer was set parallel to the film-dipping direction.

nature of the film prior to any excitation is shown by differences in $A_{||}^b$ and A_{\perp}^b in Figure 4, corresponding to absorption in the directions parallel and perpendicular to the film-dipping direction, respectively. The absorption band around 340 nm, assigned to the $\pi-\pi^*$ transition of *trans*-azobenzene,^{12,40} shows greater absorption for the polarized probe beam set parallel to the film dipping direction ($A_{||}^b$) than that in the case of the probe beam at perpendicular incidence (A_{\perp}^b). Using eq 1, the in-plane anisotropy is estimated to be $\omega = 39^\circ \pm 2^\circ$ relative to the film-dipping direction. This value is in good agreement with the angle calculated from the FTIR spectra. Other workers have also suggested that the projection components of *trans*-azobenzene moieties in the *xy* plane preferentially orient parallel to the film-dipping direction.^{18,41}

Distinct photoselection in the absorption spectra is observed when the film is illuminated for 2.5 min with the irradiation UV beam linearly polarized in the *xz* plane (the electric field parallel to the film-dipping direction). As shown in Figure 4, a clear decrease of the $\pi-\pi^*$ band was detected along the polarization direction ($A_{||}^a$), while no significant spectral change was obtained in the orthogonal direction (A_{\perp}^a). Considering the same polarized irradiation, polarized UV-visible spectra were also recorded as a function of angle by rotating the polarizer in the *xy* plane from 0° (along the *x* axis) to 360° . The yield of trans \rightarrow cis photoisomerization can be estimated by the decrease in the absorbance of the $\pi-\pi^*$ transition band (340 nm in this work) after UV irradiation. The in-plane selective conversion process can be characterized by a parameter²⁴

$$C(\theta) = 100[A_{\theta}^b - A_{\theta}^a]/A_{\theta}^b \quad (2)$$

Here θ is the angle between the polarized plane of the UV measurement and the film dipping direction. The absorbances of the 340 nm band before and after polarized UV irradiation as a function of the angle θ are expressed as A_{θ}^b and A_{θ}^a , respectively. The result (see inset in Figure

(36) Kawai, T.; Umemura, J.; Takenaka, T. *Langmuir* **1990**, *6*, 672.

(37) Schoondorp, M. A.; Schouten, A. J.; Hulshof, J. B. E.; Feringa, B. L. *Langmuir* **1993**, *9*, 1323.

(38) Walsh, S. P.; Lando, J. B. *Langmuir* **1994**, *10*, 246.

(39) Xu, X.; Kawamura, S.; Era, M.; Tsutsui, T.; Saito, S. *Nippon Kagaku Kaishi* **1987**, *11*, 2083.

(40) Griffiths, J. *Chem. Soc. Rev.* **1972**, *1*, 481.

(41) Kawaguchi, T.; Iwata, K. *Thin Solid Films* **1990**, *191*, 173.

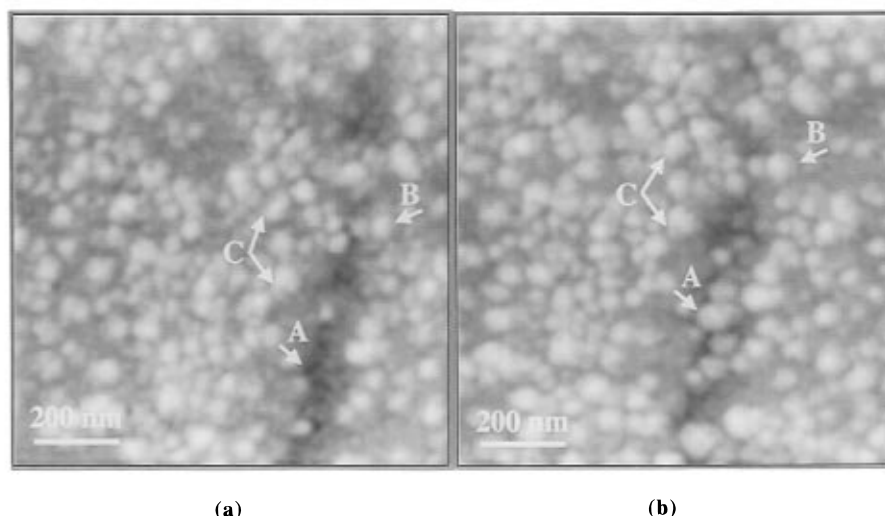


Figure 5. Morphology of the ABD LB film before (a) and after (b) 6 min. of unpolarized UV irradiation ($1000 \text{ nm} \times 1000 \text{ nm}$, "constant force" in non-contact mode).

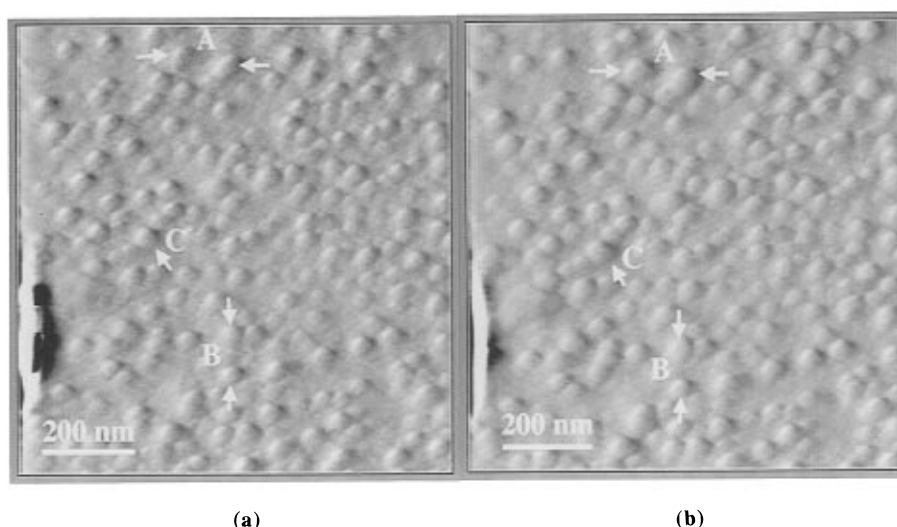


Figure 6. Morphology of the ABD LB film before (a) and after (b) 6 min of polarized UV irradiation, with the polarization direction parallel to the film-dipping direction (parallel to the scanning direction) ($1000 \text{ nm} \times 1000 \text{ nm}$, "constant height" in contact mode).

4) shows that the photoisomerization is maximized along the polarization direction of the irradiation beam.³¹ The observation indicates that the trans-ABD is converted to the cis-ABD with the highest probability for those azobenzene moieties which have transition moments whose in-plane projections are parallel to the polarization plane of the UV illumination beam, whereas the trans-ABDs with uncorrelated orientations are hardly influenced. Such a selected photoisomerization has been observed for both short time³⁰ (less than 1 min) and prolonged³¹ (more than 1 min) UV irradiation.

AFM images before and after UV irradiation were acquired for further insight into photoisomerization in ABD LB films. Films were first exposed to UV irradiation for a short time of 20 s. However no remarkable image variation was observed due to the low conversion yield (5%). Figure 5 illustrates the same area on a sample before (Figure 5a) and after (Figure 5b) 6 min unpolarized UV irradiation. The corresponding positions are recognized in the two images (A–C), although some slight drift is evident from the figures. This drift resulted from the withdrawal of the tip during UV irradiation, which was done in order to prevent the tip and the cantilever from interfering with the uniform exposure of the scanned area to the UV beam. To help to identify the structures concerned, a defect-rich, riftlike area was selected (A).

After illumination, it is easily recognized that all of the grains enlarged. In particular, several new grains, which are thought to lie within the next deeper layer, appeared within the defect-rich area (A). As is well-known, the trans \rightarrow cis photoisomerization causes an increase in the area per molecule in the LB film due to the change in molecular configuration.⁴² The expansion of the grain indicates the occurrence of photoisomerization. The structural modifications in the image suggest that, during the unpolarized UV irradiation, trans \rightarrow cis photoisomerization is induced in each grain. The reaction occurs not only on the surface layer of the film but also in deep layers of the film. The examination of the absorption spectrum in the nine-layer films and in a monolayer indicates that the photoisomerization is induced throughout all nine layers.

When polarized UV irradiation was applied to an ABD film for 6 min (Figure 6), with the electric field parallel to the film-dipping direction (parallel to the scanning direction), neighboring grains showed distinctly different behavior. As determined from these images, after polarized UV irradiation, two of the grains in region A expanded 15% in area, with an accompanying decrease in the

(42) Nakahara, H.; Fukuda, K.; Shimomura, M.; Kunitake, T. *Nippon Kagaku Kaishi* **1988**, 7, 1001.

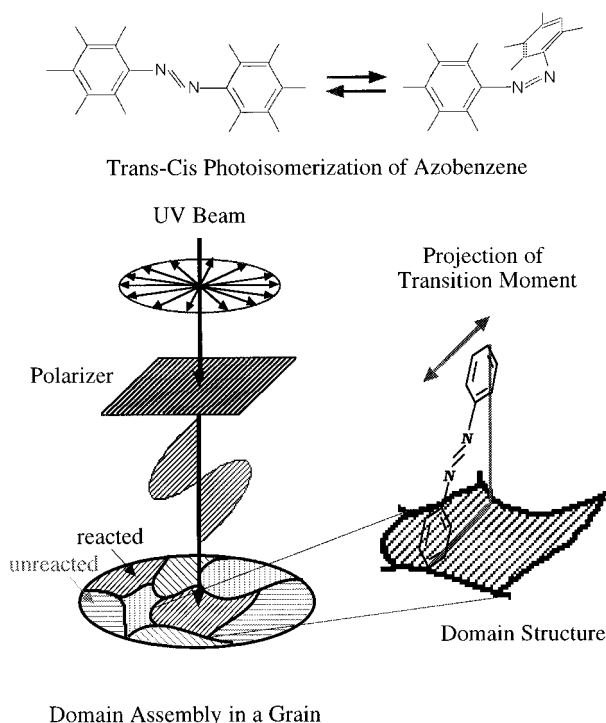


Figure 7. Schematic illustration of domain assembly and the proposed selective photoisomerization mechanism in ABD LB films.

intergrain distance. In the case of region B, two grains were observed to have similar sizes prior to illumination. However after irradiation, the upper grain expanded 36% in area, whereas the lower grain expanded only 9%. This observation strongly indicates selective photoisomerization. In the ABD LB film, domain structure was also acquired on top of the grains. However, the domain size was uncertain due to the unclear image. The average grain size was around 33 nm in diameter, which is much larger than the normal size (5–10 nm) of domains in assembled organic films.^{43–45} The phenomenon shown in Figure 6 allows us to propose the following, as illustrated in Figure 7: that a grain might be composed of several domains oriented in individual directions. The transition moments of the chromophores in the same domain, based on the in-plane projections of the molecules in that domain, are presumed to all point in approximately the same direction, but the in-plane projections of transition moments in different domains may orient in quite different directions, however.^{43,46} Domains containing molecules with in-plane projections of transition moments dominantly parallel to the polarization plane of the UV illumination beam are subject to *trans* → *cis* photoisomerization.² Since molecules inside each domain are assumed to be in an ordered structure, with strong cohesive energy, each domain is relatively independent of the neighboring domains. This causes the domains containing molecules in uncorrelated orientations with respect to the polarized UV irradiation to be scarcely influenced. When polarized light is introduced to the film, grains containing a large proportion of domains with their molecular orientations in the polarization direction of the irradiating beam may show significant enlargement in size because

of the variation of the molecular configuration from *trans*-azobenzene to *cis*-azobenzene. However, grains containing a smaller proportion of correlated domains may display smaller changes. The enlargement of the grain is thus indicative of the relative content of domains with their main molecular orientation parallel to the plane of polarization of the UV light. The selective conversion process is confirmed by the fact that some of the grains show a relatively large degree of expansion whereas others maintain their individual sizes after the irradiation. Another significant piece of evidence for this interpretation is shown in region C. After exposure to polarized light, only one grain (indicated by the arrow) expanded greatly in size; however, the surrounding grains hardly changed. This strongly supports the selectivity of the photoisomerization process in the ABD LB film.

A sequence of in situ AFM images was acquired during continued UV irradiation with either unpolarized or polarized light. With unpolarized light, almost all of the grains simultaneously showed gradual expansion at a similar rate. This implies a uniform photoisomerization process. On the contrary, with polarized light, a large proportion of the grains displayed gradual expansion but at quite different rates, while several grains remained essentially unchanged throughout the exposure to polarized UV light. This is attributed to the random distribution of domains in each grain; hence, different grains possess various compositions of domains along distinct directions. This observation further confirms the selectivity of the photoisomerization process in polarized light.

According to the above results, under unpolarized UV irradiation, *trans* → *cis* photoisomerization is induced in each domain, irrespective of the alignment of the transition moments of the chromophores; under polarized UV irradiation, however, the transformation is mainly induced in domains which are composed primarily of ABD molecules whose individual orientations of the projections of their azobenzene π – π^* transition moments are parallel to the plane of polarization of the UV illuminating beam. This process is reflected in the selective expansion of grains in polarized light. This result yields the conclusion that, during the photoisomerization, each domain can be regarded as a reacting unit in the ABD LB film.

Conclusions

The morphology of an as-transferred nine-layer ABD film was investigated with AFM in conjunction with FTIR spectroscopy. The film was composed of grains with an average area of 1100 nm². Each grain is proposed to be formed from several domains, with different overall orientations, which are joined together continuously. A unit cell with a slightly distorted monoclinic crystal structure was deduced from the molecular resolution AFM image and the linearly polarized FTIR spectra. Molecules appear to be tilted, with an average angle of $39^\circ \pm 2^\circ$ with respect to the film surface normal. Polarized UV–visible spectroscopy demonstrated that, with linearly polarized UV irradiation, *trans* → *cis* photoisomerization can be induced exclusively along a distinct polarization direction. A consistent selective photoisomerization process was revealed in real space by in situ AFM. It was inferred that each domain can be regarded as a reacting unit in the photoisomerization process. Thus the selectivity is associated directly with the domain structure in the film.

Acknowledgment. This work was partially supported by a grant from Ministry of Education, Science and Culture of Japan. One of the authors (R.W.) thanks the Iwatani Naoji Foundation for financial support.

- (43) Bourdieu, L.; Ronsin, O.; Chatenay, D. *Science* **1993**, *259*, 798.
- (44) Chidsey, C. E. D.; Bertozzi, C. R.; Putvinski, T. M.; Muijsce, A. M. *J. Am. Chem. Soc.* **1990**, *112*, 4301.
- (45) Delamarche, E.; Michel, B.; Gerber, Ch.; Anselmetti, D.; Güntherodt, H.-J.; Wolf, H.; Ringsdorf, H. *Langmuir* **1994**, *10*, 2869.
- (46) Garnes, J.; Schwartz, D. K.; Viswanathan, R.; Zasadzinski, J. A. N. *Nature* **1992**, *357*, 54.